

Emulating an Optical Planetary Access Link with an Aircraft

Abhijit Biswas,^{*a} Joseph Kovalik,^a
Martin W. Regehr,^a Malcolm Wright^a

^aJet Propulsion Laboratory, California Institute of Technology, 4800 Oak Grove Drive, Pasadena, CA. 91109,

ABSTRACT

Video imagery was streamed from the ground to an aircraft using a free-space laser communication link. The link operated at 270 Mb/s over slant ranges of 5-9 km in day and night time background conditions. The experiment was designed to demonstrate autonomous link acquisition and served as a first proof-of-concept for a planetary access link between a surface asset and an orbiter at Mars. System parameters monitored during the link demonstration including acquisition and tracking and communication performance are discussed.

Keywords: Ground-to-aircraft; streaming video; free-space laser communication

1. INTRODUCTION

In this paper the results of a ground-to-aircraft free-space laser communication link experiment are presented. The experiment was undertaken to emulate a free-space optical link between a Mars landed asset and a spacecraft orbiting Mars. We refer to this as an optical planetary access link. Most science data sent from the Mars surface to Earth since the Mars Pathfinder Mission flown in 1997, have utilized UHF access links¹ operating at instantaneous rates up to 256 kilobits per second (kb/s), with plans for 1 megabit per second (Mb/s) in the near future. Further bandwidth expansion, for example, to 30 Mb/s needed for transferring compressed high definition imagery would require higher frequencies such as X- or Ka-band and high-gain antennae² needing steering.

We are proposing optical access links with electrical power consumption and mass allocation comparable to currently used UHF systems but with 10 to 100 times higher data rates. Preliminary analysis and initial experiments to support this concept were previously reported^{3,4}. While emulating the conditions of a Mars access link is difficult, the ground-to-aircraft experiment reported herein, served as an initial proof-of-concept for a Mars optical access link.

A pair of prototype optical transceiver's, were developed for the demonstration. A description of these optical transceivers is presented in a companion paper⁵ in this volume. A Cessna 206 aircraft operated under contract to JPL by I K Curtiss Services Inc. and flying out of Burbank airport served as the airborne platform. The airborne optical transceiver was deployed inside the aircraft and line-of-sight to the ground-based transceiver was established through an acrylic window of the starboard side door. While this arrangement imposed field-of-regard limitations, it was the only viable choice given practical budget and schedule constraints.

In keeping with the theme of emulating an optical access link for a Mars scenario, we emphasized high-rate and volume data transfer from the ground to the aircraft. This is a somewhat unique feature of our link demonstration compared to other recently reported aircraft-to-ground free-space laser communication demonstrations^{6,7}. The key accomplishment of our link emulation was the successful streaming of live-video from the ground to the aircraft. Furthermore, quasi-autonomous link acquisition was implemented based on the aircraft "knowing" the ground transceivers global positioning system (GPS) location but without the ground transceiver requiring any knowledge of the aircraft's spatial location.

Infusing optical technology to provide enhanced bandwidth service of currently implemented UHF access links at Mars has several different facets. These include (i) the development of low-complexity optical transceiver hardware that can be flown to Mars while withstanding the rigors of launch from Earth and landing on Mars; (ii) design of a signaling

* abiswas@jpl.nasa.gov; phone (818)-354-2415; fax 818-393-6142; www.jpl.nasa.gov

scheme with suitable protocols and data processing and (iii) autonomous concept of operations. The aircraft link demonstration described primarily addresses the autonomous concept of operations.

In Section 2 the concept of operations for the ground-to-aircraft link with rationale for how it emulates a Mars optical access link is discussed. Key results of the link emulation are presented in Section 3. Concluding remarks are made in Section 4.

2. CONCEPT OF OPERATIONS

Mars optical access links will utilize transceivers deployed on a landed asset (rover or lander) and on the orbiter. A typical science spacecraft orbiting at altitudes of 300-400 km, for example, the Mars Reconnaissance Orbiter (MRO) will encounter link ranges between 300 and 1000 km. On the other hand, future higher-altitude telecommunication orbiters² may involve ranges of 12000 km or more.

The proposed link operations concept assumes that the Mars landed transceiver (LT) needs no knowledge of the orbiter's location. Conversely, the orbiter transceiver (OT) has sufficient position and attitude knowledge to "blind-point" a laser beam to illuminate the LT on the surface of Mars. The LT senses the OT's laser with a wide field-of-view (WFOV) camera, covering 360° in azimuth angle and ± 80° in elevation. Spectral filtering on the receive path together with image processing based on frame differencing, and centroiding are used to detect the moving orbiter's laser spot in the presence of prevalent background and to locate the OT to within ±1°. The co-ordinates are passed to a 2-axis gimballed optical head that acquires and locks on to the OT's laser beam and subsequently transmits a data-modulated uplink laser. The OT then receives data and simultaneously switches from "blind-pointing" to "closed-loop" tracking while line of sight is maintained. The WFOV camera continues to sense the downlink beam and can support re-acquisition if needed.

In our experiment a stationary ground transceiver is used to emulate the LT and the airborne transceiver functions as the OT. Figure 1 shows a schematic representation of optical link experiment.

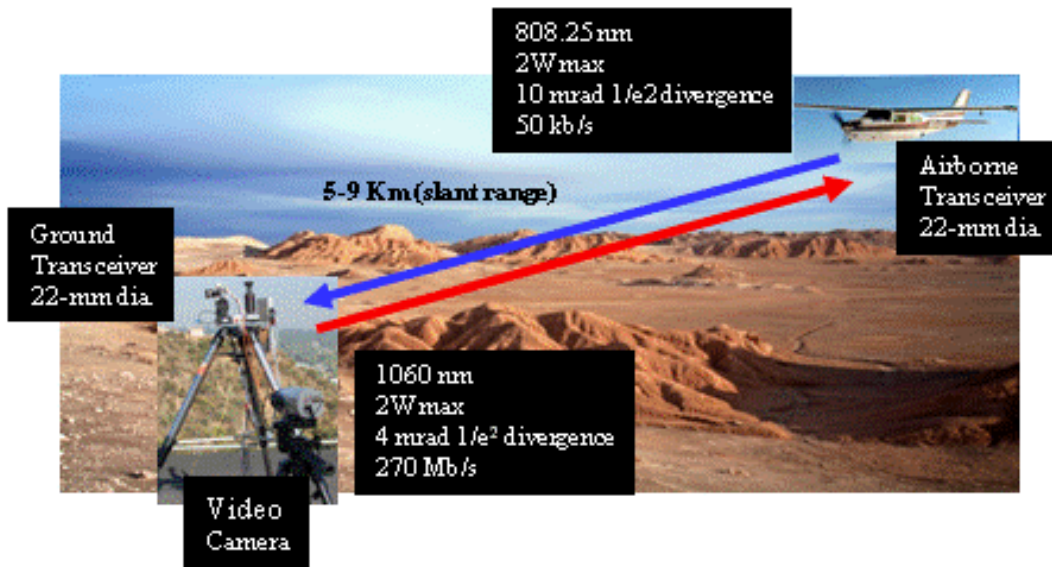


Figure 1. Overview of the optical link experiment

Emulation experiments were conducted with a ground transceiver located at JPL's Table Mountain Facility (TMF) in Wrightwood, CA and the Mesa Antenna Measurement Facility located on JPL's main campus in Pasadena. A video camera co-located with the ground transceiver was used as a data source for streaming imagery that was uplinked to the aircraft. Laser safety practices for outdoor beam transmission were followed under the guidance and supervision of JPL's System Safety Program Office. The aircraft was flown at altitudes of 7000 feet above ground level (AGL) where the aircraft made circular passes resulting in slant ranges of 5-9 km.

The optical link was bi-directional with a multi-mode fiber-coupled 808.25 nm diode laser transmitter on the aircraft transceiver. This laser was modulated at low rates to transmit data rates of 50 kb/s. The maximum laser power at 808.25

nm was 2W. A master oscillator power amplifier (MOPA) laser with a 1060 nm seed laser diode served as a laser transmitter on the uplink with a maximum single mode laser output power of 2 W. These laser wavelengths were chosen with transmission through the dust laden Mars atmosphere in mind⁴.

A photograph of the optical transceiver and its deployment on the aircraft is shown in Figure 2. Stacked transmit and receive apertures are shown mounted on the gimbal. Direct current (DC) brushless motors and encoders were used to build the custom gimbal shown. A 22 mm diameter receiving aperture and an 11 mm diameter transmitting aperture, for 1060 nm and 808.25 nm are mounted on the two-axis gimbal. The 808.25 nm multi-mode fiber is coupled to the transmitting aperture designed to emit a 12-mrad full $1/e^2$ divergence laser beam. The receiving aperture has a 10 nm bandpass spectral filter centered at 1060 nm. The received 1060 nm signal is split between a near infrared enhanced (NIR) silicon avalanche photodiode (APD) with a field-of-view (FOV) of ± 5 mrad and a silicon complimentary metal oxide semiconductor (CMOS) camera with a ± 22 mrad FOV. The APD receives either streaming digital video at 270 Mb/s or a pseudo-random binary sequence (PRBS) at 200 Mb/s. In video mode, the streaming video is stored on a video recorder (VCR) while in PRBS mode a bit-error rate tester (BERT) logs errors. In both modes the raw APD current can be monitored with a fast digital storage oscilloscope (DSO) and with a 5 kHz analog to digital converter (ADC).

The wide angle camera in Figure 2a with a field-of-view (FOV) of $\pm 10^\circ$ is not integrated to the servo loop of the transceiver but serves as an operator aid during the experiment and the video output from this camera is simultaneously recorded with a second cockpit camera (not shown) and the uplink when the link is being operated. The OT integrated to the aircraft is shown in Fig. 2b with the door open (upper panel) and through the window with the door closed (lower panel). The instrument rack used to house the processor, electronics and power-supplies is shown in the upper panel of Fig. 2b.

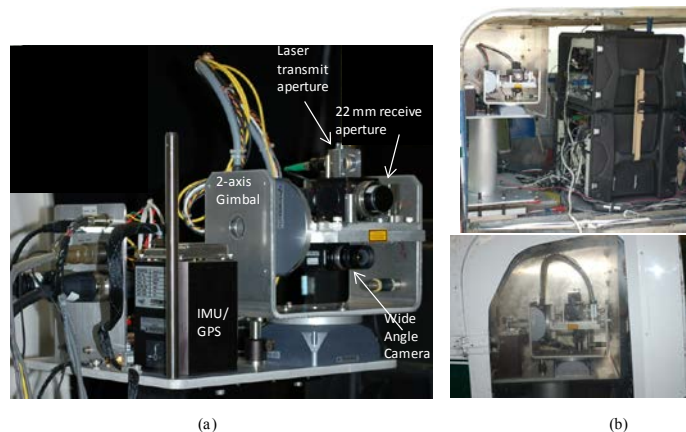


Figure 2. (a) A photograph of the OT where the laser transmitter (obscured in photograph) is integrated to the non-moving base of the gimbal; (b) The OT integrated to the aircraft with instrument rack viewed through the open side door (upper panel) and through window attached to side door (lower panel).

A global positioning system (GPS)-assisted inertial measurement unit (IMU) is integrated to the airborne transceiver. This unit allows the aircraft transceiver to monitor its position and attitude at update rates of 2-Hz. This information is processed and utilized to generate commands to the gimbal for “blind-pointing” the laser to a pre-defined GPS location on the ground. This is a key capability based upon which the quasi-autonomous operations are implemented. By providing the airborne transceiver knowledge of the ground transceivers GPS co-ordinates, the aircraft is able to illuminate the ground transceiver when the aircraft arrives at the location of the experiment and within the 5-9 km slant range. Whereas the ground transceiver does not need aircraft position but merely waits to be illuminated by the laser beam downlinked from the aircraft.

A photograph of the field deployed ground transceiver is shown in Fig. 3. Note that an instrument rack similar to that shown in Fig. 2b is used but is not shown in the photograph. The ground transceiver has a fixed wide-angle lens ($\pm 180^\circ$

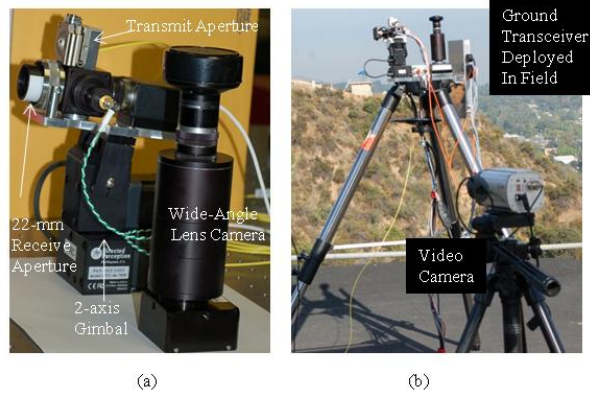


Figure 3. Photograph of (a) the ground transceiver (GT) optical head and gimbal assembly; (b) GT deployed on tripod at JPL Mesa Antenna Test Facility with a video camera providing the signal that is uplinked to the aircraft.

azimuth by $\pm 90^\circ$ in elevation) coupled to a silicon camera. A commercial fish-eye lens with an effective entrance aperture diameter of 0.7 mm was utilized. This lens is custom coupled to the camera in a manner that allows spectral filtering of the incoming light with a 2 nm band-pass centered at 808.25 nm. Upon being illuminated by the 808.25 nm laser from the aircraft the wide-angle camera senses and spatially locates the aircraft using a combination of frame-differencing and centroid computation. Aircraft co-ordinates are passed to the gimballed optical head⁴ with an accuracy of $\pm 1^\circ$. The gimballed optical head with a field-of-view (FOV) of ± 22 mrad then acquires the aircraft beacon and establishes lock prior to transmitting the 1060 nm laser modulated with high-rate data.

When the aircraft transceiver receives the 1060 nm laser from the ground it switches from “blind pointing” to a closed loop servo mode and transmits a low-rate 50 kb/s pseudo-random bit sequence to the ground. This low-rate data is received by the ground transceiver using a ± 5 mrad FOV detector. Should the link be interrupted the wide-field camera will autonomously re-acquire the link using the sequence just described.

3. EXPERIMENT AND RESULTS

3.1. Experimental Conditions

Representative experimental data are presented next. Daytime demonstrations at sun separation angles of 54° were successfully demonstrated. The estimated sky radiance for successful link acquisition on Sept. 9, 2009 (4:15 – 6:00 PDT) was $9E-4$ to $1.3E-3$ W/cm²/sr/ μ m. For the daytime links we utilized a CCD camera with the WFOV camera and at shallower Sun angles near grazing incidence caused scattered Sun light to saturate the pixels with “bleeding”. Based on sunlit sky exposures taken with a CMOS camera we believe that the exclusion angle around the Sun can be reduced to $\pm 25^\circ$, though we did not have the opportunity to demonstrate this.

The circular passes of the aircraft over the ground transceiver located at TMF and recorded by the GPS on-board the aircraft on Sept. 9, 2009 is shown in Figure 4a. The slant ranges computed from the known ground co-ordinates and aircraft altitude are shown in Figure 4b. The ground transceiver gimbal’s azimuth scan range of $\pm 150^\circ$ resulted in approximately 300-400 seconds of contact time per circular overhead pass.

The IMU on-board the aircraft also logged the roll and pitch of the aircraft at 2 Hz. Figure 5 shows a histogram of this data over the entire duration of the experiment.

Next we report on the performance and characteristics of different elements of the link demonstration. They are: (i) “blind-pointing” of the prototype orbiter transceiver (OT) or aircraft transceiver to illuminate the prototype lander transceiver (LT) on the ground; (ii) link acquisition, first by the ground-transceiver and after it points back its laser by the aircraft transceiver; (iii) tracking performance; (iv) video and pseudo-random bit-sequence transfer from the ground to the aircraft.

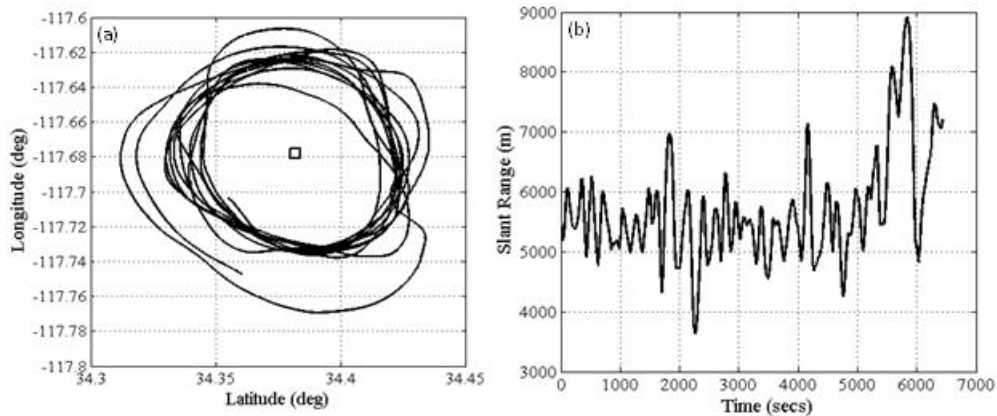


Figure 4. (a) Flight path of aircraft in latitude and longitude, the square in the center indicates the location of the LT on the ground; (b) variation of slant range of the optical link as a function of time

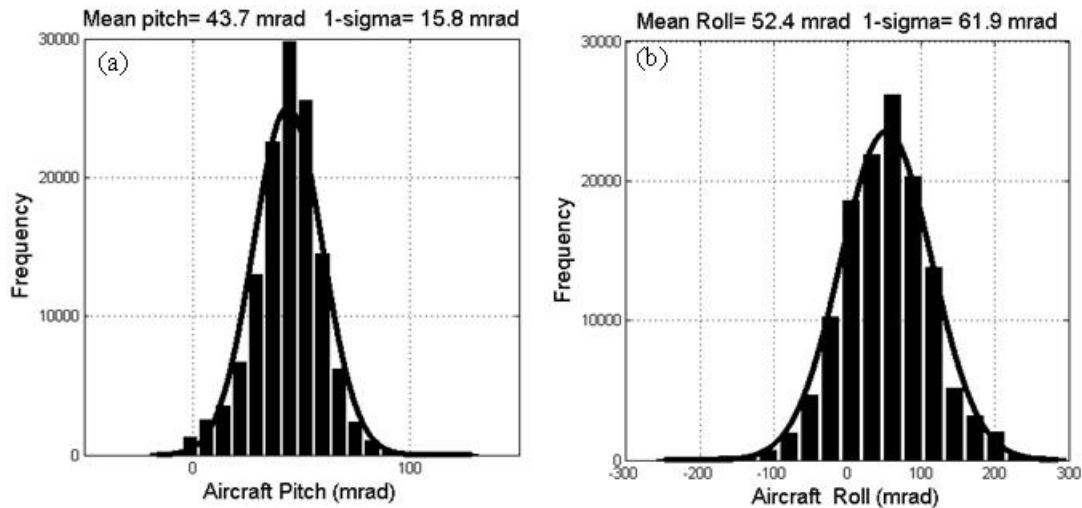


Figure 5. (a) Histogram of aircraft pitch logged by IMU the mean and standard deviation obtained using a fit (solid line) to a normal distribution are shown; (b) histogram of aircraft roll logged by IMU with the normally fitted mean and standard deviation.

3.2. Blind pointing by the OT

The blind-pointing performance was measured by disabling the aircraft transceiver servo after the link had been established, automatically transitioning the aircraft transceiver into a “blind-pointing” mode. The transmitted laser beam width from the aircraft kept the ground transceiver illuminated most of the time with the blind-pointing error, providing a reference for pointing the uplink. The motion of this uplink laser spot on the aircraft transceiver’s tracking sensor provides the blind pointing error. A scatter plot of the recorded error for a few minutes of blind-pointing is shown in Figure 6a while a time series of the centroid errors for the aircraft transceiver (shades of gray) and the ground transceiver (black) are shown in Fig. 6b. Not from Figure 6b that the error on ground transceiver error is very small for most of the duration except for a few glitches, whereas the blind pointing error recorded on the aircraft transceiver’s tracking sensor is much larger.

By fitting the measurements to a normal distribution a bias of -3.2 mrad and rms jitter of 6.6 mrad two-axis error is obtained. The errors measured are a significant fraction of the transmitted downlink beam-width. We conjecture the bias error to arise from imperfect alignment of the gimbal axes with the IMU inertial frame and could be reduced by

calibration. Our analysis also indicates that reducing the 2-Hz latency in sampling the IMU significant reduction in blind pointing jitter can be achieved suggesting that significant improvement in blind-pointing is achievable allowing transmitting much narrower beams from the aircraft.

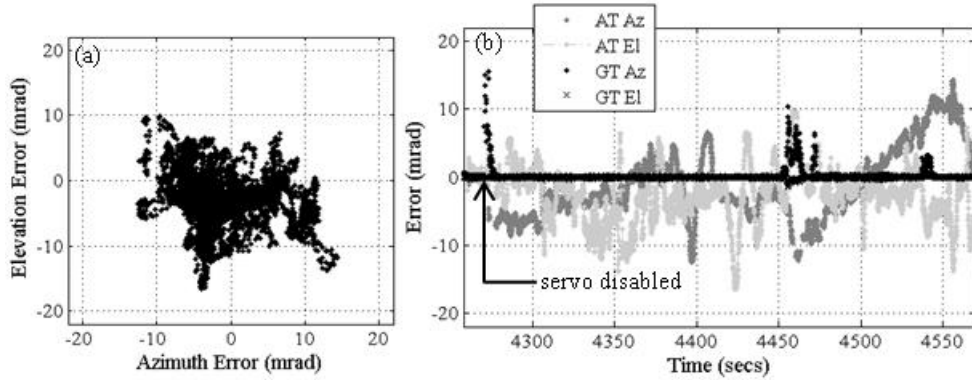


Figure 6. Measured “blind-pointing performance

3.3. Stepped link acquisition

Stepped link acquisition is initiated when the ground transceiver is illuminated by the laser blind-pointed from the aircraft. The aircraft azimuth and elevation angle can be derived from the computed centroid of the laser spot sensed by the WFOV camera. This is shown plotted against time in Fig. 7a and Fig. 7b. For the first 3 seconds the WFOV camera is sensing noise, following which WFOV camera acquires the aircraft laser as indicated by the continuous change in derived azimuth and elevation angles corresponding to motion of the aircraft. The derived azimuth and elevation angles are passed to the gimbal and after the passage of another 3 seconds the gimbal azimuth and elevation angles converge (within $\pm 1^\circ$) with the derived values from the WFOV camera. This marks the onset of downlink acquisition by the tracking camera mounted on the gimbal. Note that prior to acquisition the gimbal angles are not being updated. Following acquisition that the azimuth is steadily changing whereas the elevation angle is nearly flat because the aircraft is flying at more or less a constant altitude over the duration plotted in Figure 7a and Fig. 7b.

Figure 7c shows the tracking error derived from the centroid of the downlink laser spot on the gimbal mounted tracking camera on the ground transceiver. From initial acquisition to achieving line-of-sight stabilization takes approximately 4 seconds. Finally, in Fig. 7d a record of the centroid of the uplink laser received by the tracking camera on the aircraft transceiver is shown. Note that acquisition of the uplink occurs simultaneously with the onset of line-of-sight stabilization by the ground transceiver and takes an additional 3 seconds to settle on the aircraft.

3.4. Ground transceiver tracking error

The tracking performance monitored by logging the centroid offsets on the ground and aircraft tracking sensors are shown in Figure 8 as scatter plots. The measurements fitted to a normal distribution provided the rms errors of < 100 microradians for the ground transceiver and approximately 350 microradians for the aircraft transceiver. The higher tracking error on the aircraft is expected due to the more severe disturbance of the aircraft. Moreover, the elevation error was always worse than the azimuth and we correlate this to the large variance in roll angles shown in Figure 5b. We also observed that the jitter errors on both the ground and aircraft get worse with increased wind speeds. The worst jitter errors measured on the ground and aircraft were 150 microradians and 600 microradians when the average wind speed was 10 mph with gusts upto 25 mph.

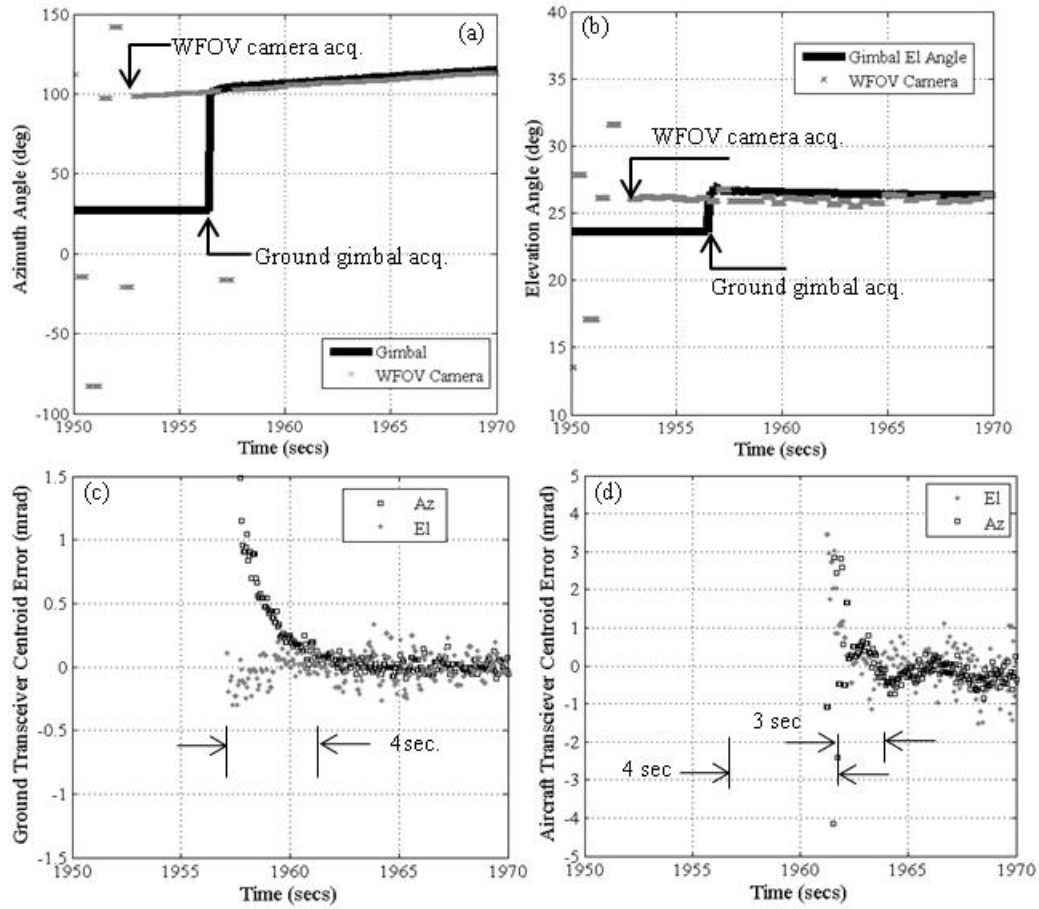


Figure 7. (a) Angular position of aircraft on WFOV camera and gimbal during acquisition by LT (b) acquisition time for LT ; (c) scatter plot of the recorded elevation and azimuth angular errors during blind-pointing.

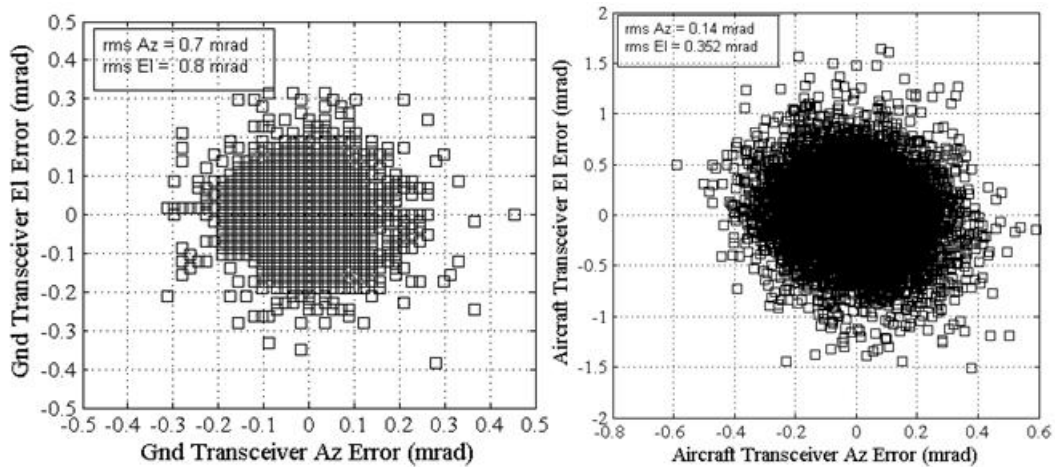
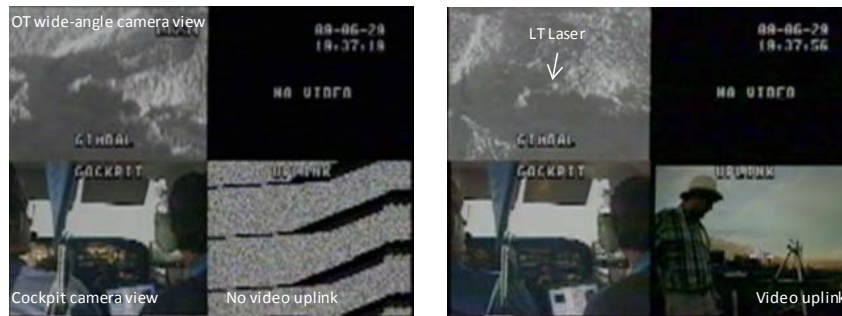


Figure 8. (a) OT closed loop tracking error scatter plot and (b) LT tracking error scatter plot.

3.5. Video and communications performance

The output from the video camera on the ground (see Figure 3b) was converted to a 270 Mb/s standard digital interface (SDI) using a commercial converter and used for modulating the uplink laser. The uplink received by the APD receiver on the aircraft was fed to SDI-to-analog video converter. The resulting output was displayed on a monitor in the cockpit, as well as recorded through one of the four quad multiplexer inputs. Two other channels of the multiplexer recorded the video output of the wide angle camera mounted on the gimbal and a cockpit camera. Figure 9 shows two frozen frames of the video recorded on the aircraft. The left frame is without uplink video while the right frame shows the uplinked video from the ground. Three of the four displayed channels were recorded. The upper left panel correspond to a record of the wide-angle camera on the aircraft transceiver that images the scene along the optical axis of the aircraft transceiver. The lower left panel is a record of the cockpit camera. The lower right panel records the uplink received from the ground. A 21-second video is included. The first 5 seconds recorded are prior to the link being established showing the lower right panel blanked out. 5-7 seconds into the video clip link acquisition is initiated and the ground laser can be seen flashing through the wide angle camera (upper left panel) as the video is acquired and stabilized. The remaining duration of the video clip shows the uplink received at the aircraft.



Video 1 Figure 9. Left still frame without uplink video compared to right frame with uplink video. <http://dx.doi.org/doi.number.goes.here>

Fig. 10a shows a sample “eye-pattern” recorded on the DSO while receiving a 200 Mb/s PRBS PN7 pattern. The unencoded bit-error rate averaged at 1-Hz is shown in Fig. 9b. Comparing links in the lab under identical transmit and receive powers, a BER of 10^{-4} on the PRBS channel was sufficient to provide high quality images with no discernible degradation on the un-encoded digital video channel. As shown in the BER diagram, the signal degradation, when evident, was quite abrupt. These errors caused glitches in the transmission of the video as well. The un-encoded bit error rates observed would not be acceptable for a robust communication channel, however, we believe that the use of a suitable code could lower the error-rate to desired levels. This was beyond the scope of our experimental objective.

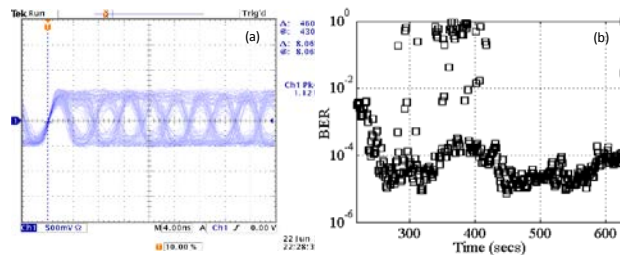


Figure 10. (a) Eye-pattern (b) unencoded BER measurement for a 200 Mb/s PRBS uplinked from the LT to the OT.

4. CONCLUSION

We presented the key findings of a ground to aircraft experiment that was intended to serve as an early proof-of-concept for a functional planetary optical access link. There was perhaps a surprising lack of mention of the impact of atmospheric turbulence on our link. We believe that the limited slant range over which the link was operated did not cause the atmospheric turbulence to pose any severe limitations. On a few experimental campaigns the normalized variance of irradiance fluctuations on the uplink, measured with 5-kHz sampling yielded scintillation indices of 0.11 suggesting weak turbulence over the slant path. Atmospheric turbulence no doubt contributed to observed performance, however, the glitches typically observed 2-3% of the time usually related to loss of pointing lock and not atmosphere induced fading.

The video transmission system used commercial converters and a simple APD receiver. The dynamic range of this receiver was limited even in laboratory testing and we point this out as another area where performance could be improved.

All in all the presumed concept of operations for a Mars optical access link was validated. Implementing such a system in Mars requires advancing technology in several key areas, most notably in low mass, power and complexity transceivers, and link layer technology utilizing efficient codes and protocols for robust reliable links. Clearly the benefit of successfully implementing low mass and power optical systems will result in 10 to 100 times enhanced data volume transfer.

ACKNOWLEDGEMENTS

The efforts of Vachik Garkanian and Carlos Esproles of JPL and Rob Burtoft of I K Curtiss Inc are gratefully acknowledged. The research described in this paper was carried out at the Jet Propulsion Laboratory, California Institute of Technology under a contract with the National Aeronautics and Space Administration.

REFERENCES

- [1] C. D. Edwards Jr., R. DePaula, "Key Telecommunications technologies for increasing data return for future Mars exploration," *Acta Astronautica*, 61, 131-138, 2007.
- [2] S. F. Franklin, J. P. Slonski Jr., Stuart Kerridge, Gary Noreen, Joseph E. Reidl, Dorothy Stosic, Caroline Racho, Bernard Edwards, Richard Austin, Don Boroson, "The 2009 Mars Telecom Orbiter Mission," *Proceedings IEEE Aerospace Conference*, Paper #1597, 2005.
- [3] Joseph M. Kovalik, Abhijit Biswas, Jeffrey R. Charles, Martin Regehr, "Autonomous access links using laser communications," *SPIE Proceedings on Free-Space Laser Communication Technologies XX1*, [Ed. Hamid Hemmati] 7199, 71990H-1 to 71990H-9, 2009.
- [4] Martin Regehr, Joseph Kovalik, Abhijit Biswas, "Acquisition and Pointing for a Mars Optical Access Link," *Proceedings IEEE Aerospace Conference*, <http://ieeexplore.ieee.org/stamp/stamp.jsp?tp=&arnumber=48393798&isnumber=4839294>.
- [5] Joachim Horwath, Christian Fuchs, "Aircraft to Ground Unidirectional Laser-Comm. Terminal for High Resolution Sensors," *SPIE Proceedings on Free-Space Laser Communication Technologies XX1*, [Ed. Hamid Hemmati], 7199, 719909-1 to 719909-7, 2009.
- [6] Larry B. Stotts, Brian Stadler, David Hughes, Paul Kolodzy, Alan Pike, David W. Young, Joseph Sluz, Juan Juarez, Buzz Graves, Dave Dougherty, Jeff Douglas and Todd Martin, "OPTICAL COMMUNICATIONS IN ATMOSPHERIC TURBULENCE," *SPIE Proceedings on Free-Space Laser Communication IX*, [Ed. Arun K. Mazumdar, Christopher C. Davis] 7464, 74603-1 to 74603-17, 2009.